DESY 94-210
November 1994

Observation of hard scattering in photoproduction events with a large rapidity gap at HERA

ZEUS COLLABORATION

HEP-EX-9501011

Abstract

Events with a large rapidity gap and total transverse energy greater than 5 GeV have been observed in quasi-real photoproduction at HERA with the ZEUS detector. The distribution of these events as a function of the γp centre of mass energy is consistent with diffractive scattering. For total transverse energies above 12 GeV, the hadronic final states show predominantly a two-jet structure with each jet having a transverse energy greater than 4 GeV. For the two-jet events, little energy flow is found outside the jets. This observation is consistent with the hard scattering of a quasi-real photon with a colourless object in the proton.

The ZEUS Collaboration

M. Derrick, D. Krakauer, S. Magill, B. Musgrave, J. Repond, J. Schlereth, R. Stanek, R.L. Talaga, J. Thron
Argonne National Laboratory, Argonne, IL, USA [p]

F. Arzarello, R. Ayad[1], G. Bari, M. Basile, L. Bellagamba, D. Boscherini, A. Bruni, G. Bruni, P. Bruni, G. Cara Romeo, G. Castellini[2], M. Chiarini, L. Cifarelli[3], F. Cindolo, F. Ciralli, A. Contin, S. D'Auria, F. Frasconi, I. Gialas, P. Giusti, G. Iacobucci, G. Laurenti, G. Levi, A. Margotti, T. Massam, R. Nania, C. Nemoz, F. Palmonari, A. Polini, G. Sartorelli, R. Timellini, Y. Zamora Garcia[1], A. Zichichi
University and INFN Bologna, Bologna, Italy [f]

A. Bargende, J. Crittenden, K. Desch, B. Diekmann, T. Doeker, M. Eckert, L. Feld, A. Frey, M. Geerts, G. Geitz[4], M. Grothe, H. Hartmann, D. Haun[5], K. Heinloth, E. Hilger, H.-P. Jakob, U.F. Katz, S.M. Mari, A. Mass, S. Mengel, J. Mollen, E. Paul, Ch. Rembser, R. Schattevoy[5], D. Schramm, J. Stamm, R. Wedemeyer
Physikalisches Institut der Universität Bonn, Bonn, Federal Republic of Germany [c]

S. Campbell-Robson, A. Cassidy, N. Dyce, B. Foster, S. George, R. Gilmore, G.P. Heath, H.F. Heath, T.J. Llewellyn, C.J.S. Morgado, D.J.P. Norman, J.A. O'Mara, R.J. Tapper, S.S. Wilson, R. Yoshida
H.H. Wills Physics Laboratory, University of Bristol, Bristol, U.K. [o]

R.R. Rau
Brookhaven National Laboratory, Upton, L.I., USA [p]

M. Arneodo, L. Iannotti, M. Schioppa, G. Susinno
Calabria University, Physics Dept.and INFN, Cosenza, Italy [f]

A. Bernstein, A. Caldwell, J.A. Parsons, S. Ritz, F. Sciulli, P.B. Straub, L. Wai, S. Yang, Q. Zhu
Columbia University, Nevis Labs., Irvington on Hudson, N.Y., USA [q]

P. Borzemski, J. Chwastowski, A. Eskreys, K. Piotrzkowski, M. Zachara, L. Zawiejski
Inst. of Nuclear Physics, Cracow, Poland [j]

L. Adamczyk, B. Bednarek, K. Eskreys, K. Jeleń, D. Kisielewska, T. Kowalski, E. Rulikowska-Zarębska, L. Suszycki, J. Zając
Faculty of Physics and Nuclear Techniques, Academy of Mining and Metallurgy, Cracow, Poland [j]

A. Kotański, M. Przybycień
Jagellonian Univ., Dept. of Physics, Cracow, Poland [k]

L.A.T. Bauerdick, U. Behrens, J.K. Bienlein, S. Böttcher[6], C. Coldewey, G. Drews, M. Flasiński[7], D.J. Gilkinson, P. Göttlicher, B. Gutjahr, T. Haas, W. Hain, D. Hasell, H. Heßling, H. Hultschig, Y. Iga, P. Joos, M. Kasemann, R. Klanner, W. Koch, L. Köpke[8], U. Kötz, H. Kowalski, W. Kröger[9], J. Krüger[5], J. Labs, A. Ladage, B. Löhr, M. Löwe, D. Lüke, O. Mańczak, J.S.T. Ng, S. Nickel, D. Notz, K. Ohrenberg, M. Roco, M. Rohde, J. Roldán[10], U. Schneekloth, W. Schulz, F. Selonke, E. Stiliaris[10], T. Voß, D. Westphal, G. Wolf, C. Youngman
Deutsches Elektronen-Synchrotron DESY, Hamburg, Federal Republic of Germany

H.J. Grabosch, A. Leich, A. Meyer, C. Rethfeldt, S. Schlenstedt
DESY-Zeuthen, Inst. für Hochenergiephysik, Zeuthen, Federal Republic of Germany

G. Barbagli, P. Pelfer
University and INFN, Florence, Italy [f]

G. Anzivino, G. Maccarrone, S. De Pasquale, S. Qian, L. Votano
INFN, Laboratori Nazionali di Frascati, Frascati, Italy [f]

A. Bamberger, A. Freidhof, T. Poser[11], S. Söldner-Rembold, J. Schroeder, G. Theisen, T. Trefzger
Fakultät für Physik der Universität Freiburg i.Br., Freiburg i.Br., Federal Republic of Germany [c]

N.H. Brook, P.J. Bussey, A.T. Doyle, I. Fleck, V.A. Jamieson, D.H. Saxon, M.L. Utley, A.S. Wilson
Dept. of Physics and Astronomy, University of Glasgow, Glasgow, U.K. [o]

A. Dannemann, U. Holm, D. Horstmann, H. Kammerlocher[11], B. Krebs[12], T. Neumann, R. Sinkus, K. Wick
Hamburg University, I. Institute of Exp. Physics, Hamburg, Federal Republic of Germany [c]

E. Badura, B.D. Burow, A. Fürtjes[13], L. Hagge, E. Lohrmann, J. Mainusch, J. Milewski, M. Nakahata[14], N. Pavel, G. Poelz, W. Schott, J. Terron[10], F. Zetsche
Hamburg University, II. Institute of Exp. Physics, Hamburg, Federal Republic of Germany [c]

T.C. Bacon, R. Beuselinck, I. Butterworth, E. Gallo, V.L. Harris, B.H. Hung, K.R. Long, D.B. Miller, P.P.O. Morawitz, A. Prinias, J.K. Sedgbeer, A.F. Whitfield
Imperial College London, High Energy Nuclear Physics Group, London, U.K. [o]

U. Mallik, E. McCliment, M.Z. Wang, S.M. Wang, J.T. Wu, Y. Zhang
University of Iowa, Physics and Astronomy Dept., Iowa City, USA [p]

P. Cloth, D. Filges
Forschungszentrum Jülich, Institut für Kernphysik, Jülich, Federal Republic of Germany

S.H. An, S.M. Hong, S.W. Nam, S.K. Park, M.H. Suh, S.H. Yon
Korea University, Seoul, Korea [h]

R. Imlay, S. Kartik, H.-J. Kim, R.R. McNeil, W. Metcalf, V.K. Nadendla
Louisiana State University, Dept. of Physics and Astronomy, Baton Rouge, LA, USA [p]

F. Barreiro[15], G. Cases, R. Graciani, J.M. Hernández, L. Hervás[15], L. Labarga[15], J. del Peso, J. Puga, J.F. de Trocóniz
Univer. Autónoma Madrid, Depto de Física Teóríca, Madrid, Spain [n]

G.R. Smith
University of Manitoba, Dept. of Physics, Winnipeg, Manitoba, Canada [a]

F. Corriveau, D.S. Hanna, J. Hartmann, L.W. Hung, J.N. Lim, C.G. Matthews, P.M. Patel, L.E. Sinclair, D.G. Stairs, M. St.Laurent, R. Ullmann, G. Zacek
McGill University, Dept. of Physics, Montreal, Quebec, Canada [a, b]

V. Bashkirov, B.A. Dolgoshein, A. Stifutkin
Moscow Engineering Physics Institute, Mosocw, Russia [l]

G.L. Bashindzhagyan, P.F. Ermolov, L.K. Gladilin, Y.A. Golubkov, V.D. Kobrin, V.A. Kuzmin, A.S. Proskuryakov, A.A. Savin, L.M. Shcheglova, A.N. Solomin, N.P. Zotov
Moscow State University, Institute of Nuclear Pysics, Moscow, Russia [m]

S. Bentvelsen, M. Botje, F. Chlebana, A. Dake, J. Engelen, P. de Jong[16], M. de Kamps, P. Kooijman, A. Kruse, V. O'Dell[17], A. Tenner, H. Tiecke, W. Verkerke, M. Vreeswijk, L. Wiggers, E. de Wolf, R. van Woudenberg
NIKHEF and University of Amsterdam, Netherlands [i]

D. Acosta, B. Bylsma, L.S. Durkin, K. Honscheid, C. Li, T.Y. Ling, K.W. McLean, W.N. Murray, I.H. Park, T.A. Romanowski[18], R. Seidlein
Ohio State University, Physics Department, Columbus, Ohio, USA [p]

D.S. Bailey, G.A. Blair[19], A. Byrne, R.J. Cashmore, A.M. Cooper-Sarkar, D. Daniels[20], R.C.E. Devenish, N. Harnew, M. Lancaster, P.E. Luffman[21], L. Lindemann, J. McFall, C. Nath, A. Quadt, H. Uijterwaal, R. Walczak, F.F. Wilson, T. Yip
Department of Physics, University of Oxford, Oxford, U.K. [o]

G. Abbiendi, A. Bertolin, R. Brugnera, R. Carlin, F. Dal Corso, M. De Giorgi, U. Dosselli, S. Limentani, M. Morandin, M. Posocco, L. Stanco, R. Stroili, C. Voci
Dipartimento di Fisica dell' Universita and INFN, Padova, Italy [f]

J. Bulmahn, J.M. Butterworth, R.G. Feild, B.Y. Oh, J.J. Whitmore[22]
Pennsylvania State University, Dept. of Physics, University Park, PA, USA [q]

G. D'Agostini, M. Iori, G. Marini, M. Mattioli, A. Nigro, E. Tassi
Dipartimento di Fisica, Univ. 'La Sapienza' and INFN, Rome, Italy [f]

J.C. Hart, N.A. McCubbin, K. Prytz, T.P. Shah, T.L. Short
Rutherford Appleton Laboratory, Chilton, Didcot, Oxon, U.K. [o]

E. Barberis, N. Cartiglia, T. Dubbs, C. Heusch, M. Van Hook, B. Hubbard, W. Lockman,
J.T. Rahn, H.F.-W. Sadrozinski, A. Seiden
University of California, Santa Cruz, CA, USA [p]

J. Biltzinger, R.J. Seifert, A.H. Walenta, G. Zech
Fachbereich Physik der Universität-Gesamthochschule Siegen, Federal Republic of Germany [c]

H. Abramowicz, G. Briskin, S. Dagan[23], A. Levy[23]
School of Physics, Tel-Aviv University, Tel Aviv, Israel [e]

T. Hasegawa, M. Hazumi, T. Ishii, M. Kuze, S. Mine, Y. Nagasawa, T. Nagira, M. Nakao, I. Suzuki, K. Tokushuku,
S. Yamada, Y. Yamazaki
Institute for Nuclear Study, University of Tokyo, Tokyo, Japan [g]

M. Chiba, R. Hamatsu, T. Hirose, K. Homma, S. Kitamura, S. Nagayama, Y. Nakamitsu
Tokyo Metropolitan University, Dept. of Physics, Tokyo, Japan [g]

R. Cirio, M. Costa, M.I. Ferrero, L. Lamberti, S. Maselli, C. Peroni, R. Sacchi, A. Solano, A. Staiano
Universita di Torino, Dipartimento di Fisica Sperimentale and INFN, Torino, Italy [f]

M. Dardo
II Faculty of Sciences, Torino University and INFN - Alessandria, Italy [f]

D.C. Bailey, D. Bandyopadhyay, F. Benard, M. Brkic, M.B. Crombie, D.M. Gingrich[24], G.F. Hartner, K.K. Joo,
G.M. Levman, J.F. Martin, R.S. Orr, C.R. Sampson, R.J. Teuscher
University of Toronto, Dept. of Physics, Toronto, Ont., Canada [a]

C.D. Catterall, T.W. Jones, P.B. Kaziewicz, J.B. Lane, R.L. Saunders, J. Shulman
University College London, Physics and Astronomy Dept., London, U.K. [o]

K. Blankenship, J. Kochocki, B. Lu, L.W. Mo
Virginia Polytechnic Inst. and State University, Physics Dept., Blacksburg, VA, USA [q]

W. Bogusz, K. Charchuła, J. Ciborowski, J. Gajewski, G. Grzelak, M. Kasprzak, M. Krzyżanowski,
K. Muchorowski, R.J. Nowak, J.M. Pawlak, T. Tymieniecka, A.K. Wróblewski, J.A. Zakrzewski, A.F. Żarnecki
Warsaw University, Institute of Experimental Physics, Warsaw, Poland [j]

M. Adamus
Institute for Nuclear Studies, Warsaw, Poland [j]

Y. Eisenberg[23], C. Glasman, U. Karshon[23], D. Revel[23], A. Shapira
Weizmann Institute, Nuclear Physics Dept., Rehovot, Israel [d]

I. Ali, B. Behrens, S. Dasu, C. Fordham, C. Foudas, A. Goussiou, R.J. Loveless, D.D. Reeder,
S. Silverstein, W.H. Smith
University of Wisconsin, Dept. of Physics, Madison, WI, USA [p]

T. Tsurugai
Meiji Gakuin University, Faculty of General Education, Yokohama, Japan

S. Bhadra[11], W.R. Frisken, K.M. Furutani
York University, Dept. of Physics, North York, Ont., Canada [a]

[1] supported by Worldlab, Lausanne, Switzerland
[2] also at IROE Florence, Italy
[3] now at Univ. of Pisa, Italy
[4] on leave of absence
[5] now a self-employed consultant
[6] now at Tel Aviv Univ., Faculty of Engineering
[7] now at Inst. of Computer Science, Jagellonian Univ., Cracow
[8] now at Univ. of Mainz
[9] now at Univ. of California, Santa Cruz
[10] supported by the European Community
[11] now at DESY
[12] now with Herfurth GmbH, Hamburg
[13] now at CERN
[14] now at Institute for Cosmic Ray Research, University of Tokyo
[15] on leave of absence at DESY, supported by DGICYT
[16] now at MIT, Cambridge, MA
[17] now at Fermilab., Batavia, IL
[18] now at Department of Energy, Washington
[19] now at RHBNC, Univ. of London, England
[20] Fulbright Scholar 1993-1994
[21] now at Cambridge Consultants, Cambridge, U.K.
[22] on leave and partially supported by DESY 1993-95
[23] supported by a MINERVA Fellowship
[24] now at Centre for Subatomic Research, Univ.of Alberta, Canada and TRIUMF, Vancouver, Canada

[a] supported by the Natural Sciences and Engineering Research Council of Canada
[b] supported by the FCAR of Quebec, Canada
[c] supported by the German Federal Ministry for Research and Technology (BMFT)
[d] supported by the MINERVA Gesellschaft für Forschung GmbH, and by the Israel Academy of Science
[e] supported by the German Israeli Foundation, and by the Israel Academy of Science
[f] supported by the Italian National Institute for Nuclear Physics (INFN)
[g] supported by the Japanese Ministry of Education, Science and Culture (the Monbusho) and its grants for Scientific Research
[h] supported by the Korean Ministry of Education and Korea Science and Engineering Foundation
[i] supported by the Netherlands Foundation for Research on Matter (FOM)
[j] supported by the Polish State Committee for Scientific Research (grant No. 204209101)
[k] supported by the Polish State Committee for Scientific Research (grant No. PB 861/2/91 and No. 2 2372 9102, grant No. PB 2 2376 9102 and No. PB 2 0092 9101)
[l] partially supported by the German Federal Ministry for Research and Technology (BMFT)
[m] supported by the German Federal Ministry for Research and Technology (BMFT), the Volkswagen Foundation, and the Deutsche Forschungsgemeinschaft
[n] supported by the Spanish Ministry of Education and Science through funds provided by CICYT
[o] supported by the Particle Physics and Astronomy Research Council
[p] supported by the US Department of Energy
[q] supported by the US National Science Foundation

1 Introduction

In a recent publication [1], it has been shown that in photoproduction at HERA energies the contribution of diffractive processes account for about 36% of the total photoproduction cross section. Diffractive processes are generally believed to proceed via the t-channel exchange of a colour-singlet object, with vacuum quantum numbers and which carries energy-momentum, called the pomeron. The true nature of the pomeron is still far from clear. Ingelman and Schlein [2] assumed that the pomeron emitted from the proton behaves like a hadron and suggested that it could have a partonic substructure which could be probed by a hard scattering process. The UA8 experiment at CERN later observed events containing two high-p_T jets in $\overline{p}p$ interactions tagged with leading protons (or antiprotons) [3]. These observations could be explained in terms of a partonic structure in the pomeron.

In previous publications [4, 5, 6, 7] evidence has been presented for events with a large rapidity gap in deep inelastic scattering (DIS). The energy dependence of the event rate as well as the approximate scaling present in the data pointed to a diffractive process of a leading twist nature. The hadronic final state of these events exhibited a small, but significant, rate for two-jet production in the $\gamma^* p$ frame. The characteristics of these events are consistent with an interaction between a virtual photon and partons in a colourless object from the proton. In this context the term 'pomeron exchange' is used as a generic name to describe the process which is responsible for creating events with a large rapidity gap.

In this paper we report the observation of events with a large rapidity gap in a sample of events with high transverse energy produced in the photoproduction regime ($Q^2 \approx 0$, where $-Q^2$ is the four-momentum transfer squared carried by the virtual photon). The analysis of the associated hadronic final states in these events includes the study of jet structure to search for a hard scattering process in diffractive photoproduction.

2 Experimental setup

2.1 HERA machine conditions

The data presented here were obtained with the ZEUS detector during the 1993 running period at the electron-proton collider HERA when 84 bunches of electrons with energy $E_e = 26.7$ GeV collided with 84 bunches of protons of energy $E_p = 820$ GeV. In addition, 10 electron and 6 proton non-colliding bunches were used for studies of beam induced background. The electron and proton beam currents were typically 10 mA.

2.2 The ZEUS detector

ZEUS is a multipurpose magnetic detector whose configuration has been described elsewhere [1, 5]. For the present analysis we used only some of the components within ZEUS. Charged particles are tracked by the vertex detector (VXD) [8] and the central tracking detector (CTD) [9] which operate inside a thin superconducting solenoid providing an axial magnetic field of 1.43 T . The solenoid is surrounded by a high resolution uranium-scintillator calorimeter divided into

three parts, forward (FCAL) covering the pseudorapidity [1] region $4.3 \geq \eta \geq 1.1$, barrel (BCAL) covering the central region $1.1 \geq \eta \geq -0.75$ and rear (RCAL) covering the backward region $-0.75 \geq \eta \geq -3.8$. The resulting solid angle coverage is 99.7% of 4π. The calorimeter parts are subdivided into towers which in turn are subdivided longitudinally into electromagnetic (EMC) and hadronic (HAC) sections. The sections are subdivided into cells, each of which is viewed by two photomultiplier tubes. The calorimeter is described in detail elsewhere [10]. For measuring the luminosity as well as for tagging the scattered electron in small Q^2 processes, we use two lead-scintillator calorimeters [11]. For these 'tagged' photoproduction events, the resulting Q^2 values are less than 0.02 GeV^2.

2.3 Trigger conditions

The data were collected with a three-level trigger. The First Level Trigger (FLT), based on a deadtime-free pipeline, selects inclusive photoproduction events with a calorimeter energy trigger. For FLT purposes, the calorimeter is subdivided into 896 trigger towers, each tower consisting of an EMC and a HAC segment. Events for this analysis were accepted by the FLT if the energy sum of EMC towers in the BCAL exceeded 3.4 GeV, or in the RCAL (excluding the cells adjacent to the beam pipe) exceeded 2.0 GeV, or the EMC towers exceeded 3.75 GeV in the RCAL towers adjacent to the beam-pipe.

The Second Level Trigger (SLT) used information from a subset of detector components to differentiate physics events from backgrounds. The SLT rejected proton beam-gas background by timing measurements in the calorimeter cells; this algorithm reduced the RCAL and BCAL FLT rates by approximately 90% and 50%, respectively.

The Third Level Trigger (TLT) had available the full event information on which to apply physics-based filters. The TLT applied stricter cuts on the event times and also rejected beam-halo muons and cosmic muons. The logic of the filter used in this analysis is described in the data selection section.

3 Kinematics of photoproduction events

In electron-proton scattering, photoproduction can be studied in the limit of small four-momentum transfer, q, carried by the virtual photon, γ^*. The kinematic variables used to describe the reaction $e\ (k)\ +\ p\ (P) \rightarrow e\ (k')\ +\ X$, are the following: the square of the total ep centre of mass energy: $s = (k\ +\ P)^2 \approx 4E_pE_e = 87576$ GeV^2; the four-momentum transfer squared carried by the virtual photon: $Q^2 = -q^2 = -(k\ -\ k')^2$; the Bjorken variable describing the energy transfer to the hadronic system: $y = \frac{q \cdot P}{k \cdot q}$; and the centre of mass energy squared of the $\gamma^* p$ system: $W^2 = (q + P)^2 = ys$.

For events with a detected electron, the variable y can be obtained from

$$y_e = 1 - \frac{E'_e}{E_e}\ \frac{1 - cos\theta'_e}{2} \qquad (1)$$

[1] The ZEUS coordinate system is defined as right-handed with the Z axis pointing in the (forward) proton direction and the X axis pointing horizontally towards the centre of the HERA rings. The pseudorapidity η is defined as $-\ln(\tan\frac{\theta}{2})$, where the polar angle θ is taken with respect to the proton beam direction from the nominal interaction point (IP).

where E'_e denotes the scattered electron energy and θ'_e the electron scattering angle. Alternatively, y can be determined approximately from the hadronic system using the Jacquet-Blondel expression

$$y_{JB} = \frac{\sum_i (E_i - p_{zi})}{2 \cdot E_e} \tag{2}$$

with the sum running over all calorimeter cells i associated with the hadronic system. We denote by E_i the energy in cell i, $p_{zi} = E_i \cdot cos\theta_i$ and θ_i is the angle of the centre of the cell with respect to the event vertex. The invariant mass, M_X, of the hadronic system detected in the ZEUS central detector is determined from the calorimeter cell information: $M_X^2 = E_H^2 - p_H^2$, where E_H and p_H are the energy and momentum of the hadronic system. Cells in the electromagnetic (hadronic) calorimeter sections with energies below 60 MeV (110 MeV) were excluded in the present analysis.

4 Data selection

The cuts to select hard photoproduction events are similar to those described in our previous publications [12, 13]. In particular, we

- reject events with an electron found in the calorimeter with an energy greater than 5 GeV and $y_e \leq 0.7$, to remove DIS background;
- require $0.05 \leq y_{JB} \leq 0.8$, to remove beam-gas and those DIS events where the scattered electron was not identified and therefore was mistakenly included in the hadronic system;
- reject events with an energy in the rear section of the calorimeter $E_{RCAL} > 30$ GeV, to remove background from non-ep collisions;
- reject events with a missing transverse momentum, $\not{p}_T > 10$ GeV/c;
- require a vertex with $-35 \leq Z \leq 20$ cm and a radial distance from the beam line $R \leq 4$ cm;
- require $\frac{\sum_i p_{zi}}{\sum_i E_i} \leq 0.9$, at least two oppositely charged tracks with $p_T \geq 0.5$ GeV, and one of the following: transverse energy in a cone outside 10^o of the forward direction in excess of 5 GeV; or $y_{JB} \geq 0.28$; or $\frac{\sum_i p_{zi}}{\sum_i E_i} \leq 0.8$; or an electron with an energy larger than 5 GeV detected in the luminosity monitor; these criteria were essential to enable us to reach lower transverse energies than in previous publications [12];
- require a total transverse energy $E_T \geq 5$ GeV.

The last condition in particular defines 'hard photoproduction' in the context of this analysis.

From an integrated luminosity of 0.55 pb^{-1}, a sample of 417081 events passed these cuts. This sample has less than a 0.1% contamination from beam-gas interactions, as determined from the number of events originating from non-colliding electron and proton bunches. The cosmic

ray background, estimated from the rate of events outside of ep bunch crossings, is negligible. The requirement that no electron is found in the ZEUS calorimeter ensures that $Q^2 \leq 4$ GeV^2. Monte Carlo studies, using the ALLM [14] prescription which provides a smooth interpolation from deep inelastic scattering to $Q^2 = 0$, show that for the accepted photoproduction events the median Q^2 is 10^{-3} GeV^2. The same Monte Carlo program predicts that 27% of the events should have a scattered electron measured in the electron calorimeter of the luminosity detector, in agreement with the observed fraction of 26.7%.

5 The Monte-Carlo simulation

The hadronic final states observed in hard photoproduction can be understood as the result of two different leading order (LO) mechanisms:

- direct processes where the photon interacts with a gluon (g) in the proton giving rise to a quark-antiquark pair (Boson Gluon Fusion) or with a quark (q), generating a qg final state (QCD Compton), and
- resolved processes [15] where a parton in the photon interacts with a parton in the proton.

Calculations of the relative importance of these two competing mechanisms at HERA energies have shown that the hard photoproduction cross section is dominated by resolved processes [16]. These expectations have been recently confirmed experimentally [12, 13, 17].

The Monte Carlo generator PYTHIA 5.6 [18] was used to model standard hard photoproduction processes. In this generator, the direct and resolved photon processes are each simulated using leading order matrix elements, with the inclusion of initial and final state parton showers. The lower cut-off on the transverse momentum of the generated final-state partons p_{tmin} was chosen to be 2.5 GeV/c. The photon parton distributions were parametrized according to GRV-LO [19] while for the proton MRSD$'_-$ [20] was used. The Weizsäcker-Williams approximation was used to describe the photon flux at the lepton vertex. This Monte Carlo simulation does not contain any explicit contribution from diffractive γp interactions.

Diffractive processes were simulated using POMPYT [21]. This is a Monte Carlo model in which, within the framework provided by PYTHIA, the proton emits a pomeron whose partonic constituents subsequently take part in a hard scattering process with the photon or its constituents. This model incorporates approximately energy independent cross sections as experimentally determined in hadron-hadron collisions.

The photon contribution contains both direct and resolved processes and the parton density distribution is parameterised according to DG [22]. The parton momentum densities of the pomeron are parameterised according to the hard distribution [2, 21]

$$\beta f(\beta) = constant \cdot \ \beta(1-\beta) \tag{3}$$

where $\beta = x_{parton/pom}$ denotes the fraction of the pomeron momentum involved in the scattering.[2] Two possibilities have been considered: one in which the partons in the pomeron are quarks

[2]The soft parton density has not been considered since it does not describe our DIS data [5].

(quarkonic pomeron) and a second one in which the partons are gluons (gluonic pomeron). The two predictions from the POMPYT model will be shown separately.

In our previous publication on the study of jet production in DIS events with a large rapidity gap, the Nikolaev-Zakharov (N-Z) model [23] gave similar results to POMPYT. For the photoproduction processes studied here, the N-Z model again gives similar results to POMPYT.

For all of the comparisons shown below, the number of Monte Carlo events has been normalised to the data in each figure and so only the shapes of the distributions may be compared. The Monte Carlo events were passed through reconstruction and selection procedures identical to those for the data.

6 Results

6.1 Events with large rapidity gaps

Following [4, 5] we define η_{max} as the maximum pseudorapidity of all calorimeter condensates in an event, where a condensate is defined as an isolated set of adjacent cells with summed energy above 400 MeV. The pseudorapidity of the condensate is then calculated from the angle of the energy weighted centre of the condensate with respect to the measured IP. The distribution of η_{max} is shown in Fig 1a. The data presented in this and all following figures are not corrected for effects from detector acceptance and smearing. The dip in the η_{max} distribution at $\eta_{max} \approx 1.1$ is a detector effect. Values of $\eta_{max} \geq 4.3$, which are outside the acceptance of the calorimeter, occur when energy is deposited in many contiguous cells around the beam pipe in the forward (proton) direction. This region is sensitive to the fragmentation of the proton remnant which at HERA energies is not yet fully understood. The bulk of the events cluster around $\eta_{max} \sim 4$ in fair agreement with the expectations of PYTHIA. In addition to this region of large η_{max} a second class of events with $\eta_{max} \leq 1.5$ is seen in the data. There are 6678 events with $\eta_{max} \leq 1.5$, corresponding to 1.6 % of the total sample. The beam-gas contamination in this subsample is less than 1% and that due to cosmic rays is 1.3%.

The shape of the distribution for $\eta_{max} \leq 1.5$ is not accounted for by standard Monte Carlo simulations for hard photoproduction processes as in PYTHIA. It is, however, in good agreement with the predictions of the POMPYT model, as illustrated in Fig. 1a. Note that the normalisations of the POMPYT and PYTHIA samples in this figure have been fixed to the number of data events below and above $\eta_{max} = 1.5$, respectively. According to POMPYT, for events with $E_T > 5$ GeV the acceptance after the $\eta_{max} \leq 1.5$ cut is about 9% (10%) for a quarkonic (gluonic) pomeron.

In Regge phenomenology for soft processes the amplitudes for two-body scattering by pomeron exchange are characterized by a constant or slowly rising dependence on W, the centre of mass energy, while reggeon exchange leads to a power law decrease. Hence, the W dependence of the rate of large rapidity gap events is a sensitive measure of the type of exchange contributing to the scattering process. It is important to study whether the same phenomenology exists for hard scattering, the subject of this paper. The distributions in $W = (y_{JB} \cdot s)^{\frac{1}{2}}$ for all events and for those with $\eta_{max} \leq 1.5$ are shown in Fig. 1b. Also shown are the POMPYT predictions for events with $\eta_{max} \leq 1.5$. The good agreement of POMPYT with the data is

consistent with the assumption that the dominant mechanism for large rapidity gap events is pomeron exchange.

The mass of the hadronic system was measured with the calorimeter as described at the end of section 3. The distribution of M_X for events with a large rapidity gap is shown in Fig. 1c. The resolution in the determination of M_X is between 10-20%. According to Monte Carlo calculations the reconstructed M_X values are typically underestimated by about 20% with respect to the generated masses. The M_X distribution is steeply falling for M_X values above 12 GeV. This is similar to the behaviour observed in DIS for events selected with similar cuts [5]. Neither the gluonic nor quarkonic POMPYT model gives a satisfactory description of the data. The correlation between M_X and η_{max} is displayed in Fig. 1d. Note that, according to POMPYT, there are diffractive events at high M_X values which are suppressed by the η_{max} cut.

If large rapidity gap events are interpreted as being due to pomeron exchange, then the fraction of the proton momentum carried by the pomeron $x_{pom/p}$ can be determined from the mass of the hadronic system via the relation

$$x_{pom/p} = \frac{M_X^2}{W^2}. \tag{4}$$

For events with $\eta_{max} \leq 1.5$, $x_{pom/p}$ clusters (not shown) around values of $\sim 3 \cdot 10^{-3}$ due to the applied cuts. The $x_{pom/p}$ values are limited on the lower side to $7{\cdot}10^{-4}$ by the $E_T \geq 5$ GeV requirement while the $\eta_{max} \leq 1.5$ cut suppresses values of $x_{pom/p}$ above 10^{-2}. Similar $x_{pom/p}$ values have been observed in DIS [5].

6.2 Jet structure

Evidence for multijet structure in hard photoproduction at HERA has been presented in [12, 13, 17]. In the events with $E_T \geq 5$ GeV a search was performed for jet structure using a cone-based jet algorithm in pseudorapidity (η), azimuth (ϕ) space [24], subject to the Snowmass convention [25]. The cone radius $R = (\Delta\phi^2 + \Delta\eta^2)^{\frac{1}{2}}$ in the algorithm was set to 1 unit. In order to ensure that for standard (non-diffractive) hard photoproduction the results are not biased by fragments from the proton remnant, whose fragmentation properties at these energies are not well known, calorimeter cells with polar angles smaller than 9° ($\eta \geq 2.5$) in the laboratory were excluded.

In the first step of the jet algorithm, each calorimeter cell with a transverse energy in excess of 300 MeV is considered as a seed for the search. These seeds are combined if their distance in $\eta - \phi$ space, R, is smaller than 1 unit. Then a cone of radius $R = 1$ is drawn around each seed and the calorimeter cells within that cone are combined to form a cluster. The axis of the cluster is defined according to the Snowmass convention: $\eta^{cluster}$ ($\phi^{cluster}$) is the transverse energy weighted mean pseudorapidity (azimuth) of all the calorimeter cells belonging to that cluster. A new cone of radius 1 unit is then drawn around the axis of the cluster. All cells inside the cone are used to recalculate a new cluster axis. The procedure is iterated until the content of the cluster does not change.

The energy sharing of overlapping clusters is then considered. Two clusters are merged if the common transverse energy exceeds 75% of the total transverse energy of the cluster with the lowest transverse enrgy; otherwise two different clusters are formed and the common cells

are assigned to the nearest cluster. Finally, a cluster is called a jet if $E_T^{cluster} \geq$ 4 GeV. The transverse energy weighted mean pseudorapidity (η_{jet}) and azimuth (ϕ_{jet}) were evaluated and jets were accepted for the present analysis if $\eta_{jet} \leq 2$, corresponding to polar angles larger than 15°.

We find that 91.4%, 6.5%, 2.0% and 0.1% of the events with total transverse energy $E_T >$ 5 GeV belong to the zero-, one-, two- and three- or more-jet categories in the sample of events with $\eta_{max} \leq 1.5$. The fraction of zero-jet events depends strongly on the jet definition, in particular on the requirement that the jet transverse energy be larger than 4 GeV.

To determine the background present in the two-jet sample with a large rapidity gap, we studied the empty as well as the non-colliding electron and proton bunches and set an upper limit of 1% for the beam-gas and cosmic ray backgrounds. For further confirmation that this sample of two-jet events is from photoproduction processes, we measured the fraction of two-jet events where the scattered electron is tagged in the electron calorimeter of the luminosity monitor with an energy between 5 and 22 GeV and for which $Q^2 < 0.02$ GeV^2. This was found to be 24% in agreement with both Monte Carlo expectations and the value for the complete high E_T photoproduction sample.

Figure 2a displays the η_{max} distribution for all events with two or more jets. A sample of 132 two-jet events with $\eta_{max} \leq 1.5$ is observed, corresponding to 0.63% of the hard photoproduction two-jet sample. This number of events is not accounted for by the standard hard photoproduction processes as modelled by PYTHIA which predicts fewer than 18 ± 7 two-jet events with $\eta_{max} \leq 1.5$. Therefore, the two-jet events observed with $\eta_{max} \leq 1.5$ are not just the tail of 'standard' hard photoproduction with two jets [12]. Both POMPYT samples give a good representation of the shape of the η_{max} distribution for these events.

For events with $\eta_{max} \leq 1.5$, the distribution of the total transverse energy per event, E_T, is shown in Fig. 2b for all events (open histogram), for events with at least one jet in the final state (cross hatched) and for those events with two or more jets (shaded). For $E_T \geq 8$ GeV, which is the minimum E_T for which two-jet production with $E_T \geq 4$ GeV is possible, 9.9% of the events are of the two-jet type. For $E_T \geq 12$ GeV the majority of the events are of the two-jet type; an example of which is shown in Fig. 2c. For two-jet events the distribution of the transverse jet energies reaches up to values of 10 GeV, as shown in Fig. 3a. In Fig. 3b the difference in azimuth ($\Delta\phi^{jet}$) of the two jets in the large rapidity gap sample is displayed. The two jets are preferentially back-to-back in the transverse plane. The predictions from both POMPYT models are in fair agreement with these data.

6.3 Transverse energy flow around the jet axis

The profiles of the jets observed in high E_T photoproduction events are compared for events with and without a large rapidity gap. Figures 3c, d show the transverse energy flows around the jet axis. To reduce the bias from the $\eta_{max} \leq 1.5$ cut, the jets for both samples were restricted to the region $\eta_{jet} \leq 0$ and calorimeter cell energy deposits with $\eta_{cell} > 1.5$ were excluded. Fig 3c shows that the E_T-weighted azimuthal distributions ($\Delta\phi = \phi_{cell} - \phi_{jet\ axis}$) in the jet core are essentially the same for the large rapidity gap events ($\eta_{max} \leq 1.5$) and for the hard photoproduction sample with $\eta_{max} > 1.5$. However, the transverse energy outside of the jet core is about a factor of two larger for the $\eta_{max} > 1.5$ sample than for the large rapidity gap events.

Figure 3d shows the E_T-weighted distribution for $\Delta\eta$, the difference in rapidity of a given calorimeter cell and the jet axis. For this figure, only energy deposits in the hemisphere containing the jet are included. The transverse energy flow in the core of the jet is the same for events with and without a large rapidity gap, indicating that the jets themselves are similar. However, jets produced in events without a large rapidity gap show at large (forward) $\Delta\eta$ values a significant E_T flow. In contrast, the jet profile for the large rapidity gap sample is more symmetric and shows a factor of two to three less E_T flow in the forward direction. These observations are similar to those presented in our previous publications on DIS events with and without a large rapidity gap [5, 6] where it was demonstrated there is a suppression of colour flow between the outgoing nucleon system and the struck parton in events with a large rapidity gap.

6.4 Momentum fractions

We conclude that we have observed large rapidity gap events containing two jets, consistent with a photon pomeron hard scattering process leading to a two-jet final state. In $2 \rightarrow 2$ parton scattering the momenta of the incoming partons can be calculated from the two partons in the final state. Let x_γ and x_p be the fractions of the photon and proton momenta carried by the initial state partons. If the final state partons are approximated by the two jets observed, energy-momentum conservation leads to the relationship:

$$x_\gamma = \frac{\sum(E - p_z)_{Jets}}{\sum(E - p_z)_{hadrons}}, \tag{5}$$

$$x_p = \frac{\sum(E + p_z)_{Jets}}{2E_p}. \tag{6}$$

In these expressions 'Jets' refers to a sum over all calorimeter cells that comprise the jets according to the cone algorithm employed. Direct photon processes are characterised by x_γ values close to 1.

Equations (5) and (6) were used to calculate x_γ and x_p. The resolutions are comparable to those reported in an earlier publication on the hard photoproduction of two jets[12] and are in the range (10-20)%. The x_γ distribution shown in Fig. 4a peaks near $x_\gamma = 1$. The sum of the direct and resolved photon contributions as calculated by POMPYT for a gluonic pomeron gives a reasonable description of the data, as does a pure direct photon interaction with a quarkonic pomeron. In contrast, the shape of a purely resolved photon contribution is inadequate to describe the data, as seen by the dashed-dotted histogram in Fig. 4a which was calculated for a quarkonic pomeron with Eq. (3).

The distribution of x_p, the fraction of the proton's momentum participating in the hard scattering, is displayed in Fig 4b and shows that most of the two-jet events have x_p values between $3{\cdot}10^{-3}$ and 10^{-2}. The low and high limits are due to the E_T and η_{max} cuts, respectively, as discussed in section 6.1. In this sample, the two jets populate the pseudorapidity region $-2 \leq \eta_{jet} \leq 1$ as shown in Fig. 4c, because the $\eta_{max} \leq 1.5$ cut suppresses jets with $\eta_{jet} > 1$.

In standard hard photoproduction at HERA, the centre-of-mass of the hard process is boosted in the proton direction and, therefore, in most two-jet events both jets go forward [12]. This is particularly true for the resolved photon process which is, in general, the dominant jet

production process at the transverse energies considered here. At centre-of-mass energies of $W \sim 200$ GeV, the direct photon process is expected to dominate only at transverse energies above 50 GeV [16]. In the selected sample of large rapidity gap events, M_X is an order of magnitude smaller than W, thus limiting the available phase space. The dominance of the direct component hence occurs at transverse energies an order of magnitude smaller than in standard hard photoproduction. Therefore the fact that two-jet events in the large rapidity gap sample are found to be mainly due to the direct coupling of the photon is well understood with the conventional parton density parametrisations of the photon. These features are reproduced by the POMPYT model.

7 Conclusions

We have observed photoproduction events with a large rapidity gap and large transverse energy at HERA. Their distribution as a function of the γp centre of mass energy is consistent with a diffractive process. Hard scattering, with jets having transverse energies greater than 4 GeV, has been observed in these large rapidity gap events. For total transverse energies above 12 GeV the hadronic final state is dominated by two-jet production with the two jets being preferentially back-to-back in azimuth. For the two-jet events selected by the cuts used in this analysis, the fraction of the photon momentum participating in the hard scattering is close to one, suggesting that their production is dominated by direct photon processes. The two-jet events in the large rapidity gap sample show little energy outside the jet core. A natural interpretation of these events is the hard interaction of the photon with a colourless object inside the proton: the pomeron. These conclusions complement those drawn from the production of large rapidity gap events in deep inelastic scattering.

Acknowledgements

We thank the DESY Directorate for their strong support and encouragement. The remarkable achievements of the HERA machine group were essential for the successful completion of this work and we are grateful for their efforts which enabled us to achieve a factor of twenty increase in the integrated luminosity for the 1993 running period over that achieved in 1992.

References

[1] ZEUS Collab., M. Derrick et al, Z. Phys. C63 (1994) 391.

[2] G. Ingelman and P. E. Schlein, Phys. Lett. B152 (1985) 256.

[3] UA8 Collab., R. Bonino et al, Phys. Lett. B211 (1988) 239; A. Brandt et al, Phys. Lett. B297 (1992) 417.

[4] ZEUS Collab., M. Derrick et al., Phys. Lett. B315 (1993) 481.

[5] ZEUS Collab., M. Derrick et al., Phys. Lett. B332 (1994) 228.

[6] ZEUS Collab., M. Derrick et al.,DESY 94-117 (July 1994) accepted by Phys. Letters B.

[7] H1 Collab., T. Ahmed et al., DESY 94-133 (July 1994).

[8] C. Alvisi et al., Nucl. Instr. Meth. A305 (1991) 30.

[9] C.B. Brooks et al., Nucl. Instr. Meth. A283 (1989) 477; B. Foster et al., Nucl. Instr. Meth. A338 (1994) 254.

[10] A. Andresen et al., Nucl. Instr. Meth. A309 (1991) 101; A. Caldwell et al., Nucl. Instr. Meth. A321 (1992) 356; A. Bernstein et al., Nucl. Instr. Meth. A336 (1993) 23.

[11] J. Andruszków et al., DESY 92–066 (1992).

[12] ZEUS Collab., M. Derrick et al., Phys. Lett. B322 (1994) 287.

[13] ZEUS Collab., M. Derrick et al., Phys. Lett. B297 (1992) 404.

[14] H. Abramowicz et al., Phys. Lett. B269 (1991) 465.

[15] E. Witten, Nucl. Phys. B120 (1977) 189.

[16] W.J. Stirling and Z. Kunszt in Proceedings of HERA Workshop (1987) 331; M. Drees and R.M. Godbole, Phys. Rev. D39 (1989) 169.

[17] H1 Collab., T. Ahmed et al., Phys. Lett. B297 (1992) 205; I. Abt et al., Phys. Lett. B314 (1993) 436.

[18] H.-U. Bengtsson and T. Sjöstrand, Comp. Phys. Comm. 46 (1987) 43; T. Sjöstrand, CERN-TH.6488/92.

[19] M. Glück, E. Reya and A. Vogt, Phys. Rev. D45 (1992) 3986.

[20] A. D. Martin, W. J. Stirling and R.G. Roberts , Phys. Lett. B306 (1993) 145.

[21] P. Bruni and G. Ingelman, Proc. of the International Europhysics Conference on High Energy Physics, ed. J. Carr and M. Perrotet, Marseille, France, July, 1993 (Ed. Frontieres, Gif-sur-Yvette, 1994), p. 595.

[22] M. Drees and K. Grassie, Z. Phys. C28 (1985) 451.

[23] N. N. Nikolaev and B. G. Zakharov, Z. Phys. C53 (1992) 331.

[24] UA1 Collab., G. Arnison et al., Phys. Lett. B123 (1983) 115

[25] J. Huth et al., FERMILAB-Conf-90-249-E.

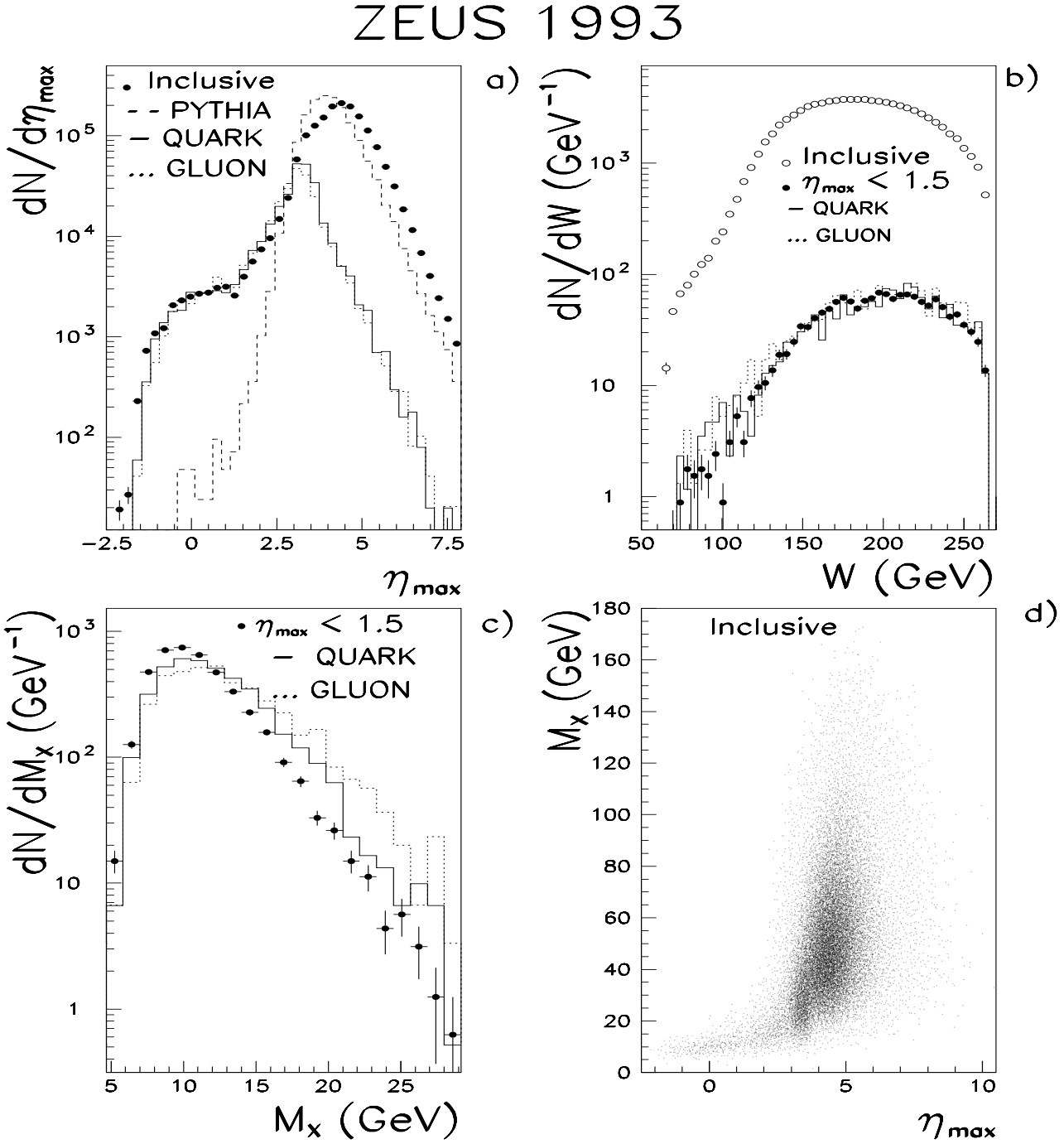

Figure 1:
(a) The distribution of η_{max}, the pseudorapidity of the most forward calorimeter condensate with energy above 400 MeV for the photoproduction sample with $E_T > 5$ GeV along with the predictions from PYTHIA (dashed line) and POMPYT with a quarkonic (solid line) or gluonic (dotted line) pomeron.
(b) The distribution in W for all events and for those with $\eta_{max} \leq 1.5$. The latter are well described by pomeron induced reactions as implemented in POMPYT.
(c) The mass of the hadronic system M_X for events with a large rapidity gap as defined by $\eta_{max} \leq 1.5$ along with the POMPYT predictions.
(d) A scatter plot of the mass of the hadronic system, M_X, versus η_{max}.

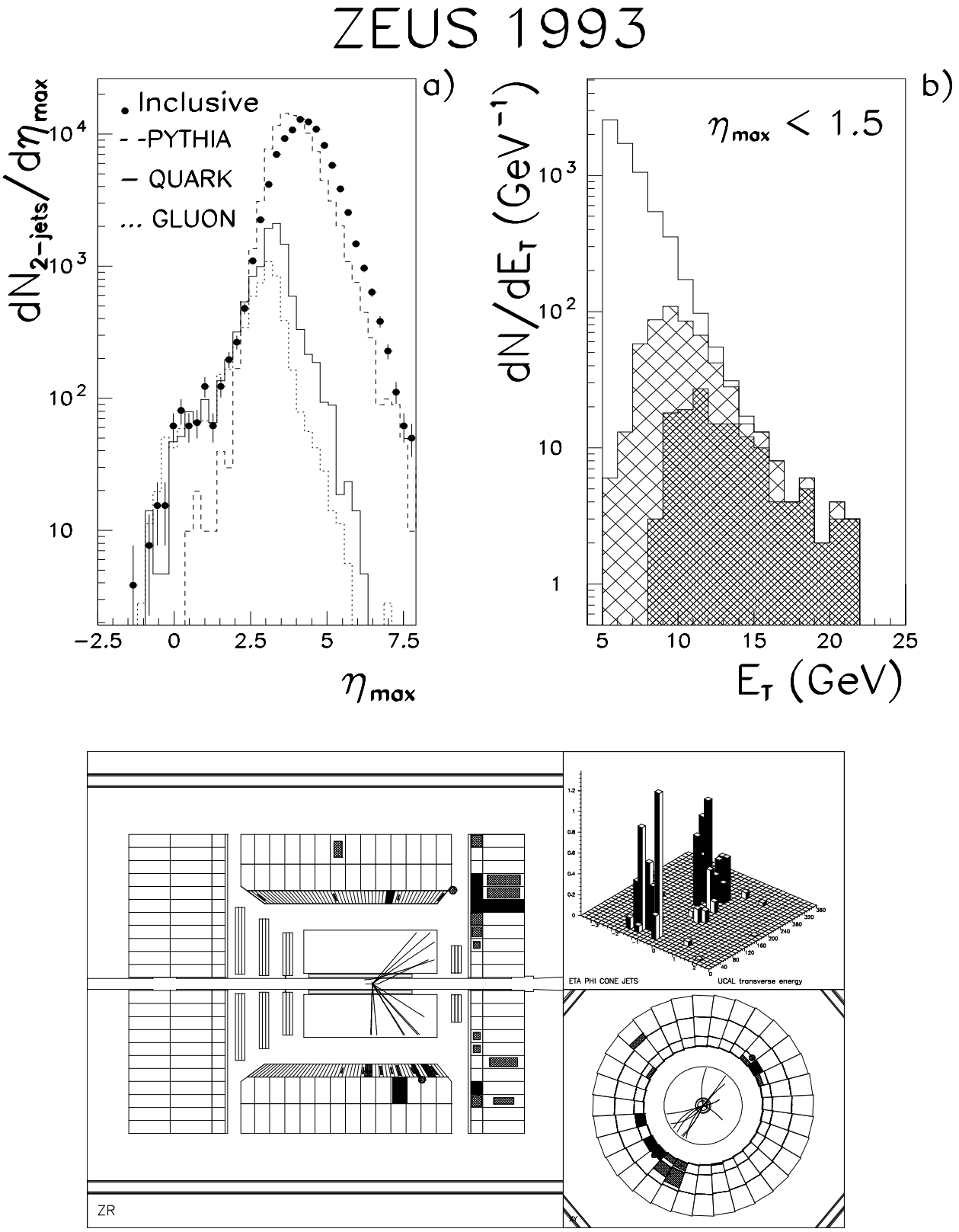

Figure 2:
(a) The distribution of η_{max} in the photoproduction sample with $E_T > 5$ GeV and two or more jets along with the predictions from PYTHIA (dashed line) and POMPYT with a quarkonic (solid line) or gluonic (dotted line) pomeron.
(b) The distribution of the total transverse energy E_T for the photoproduction sample with a large rapidity gap and, in addition, for the subsample of those events with at least one (cross hatched area) and at least two (shaded area) jets in the final state.
(c) A display of a two-jet event in hard photoproduction with a large rapidity gap.

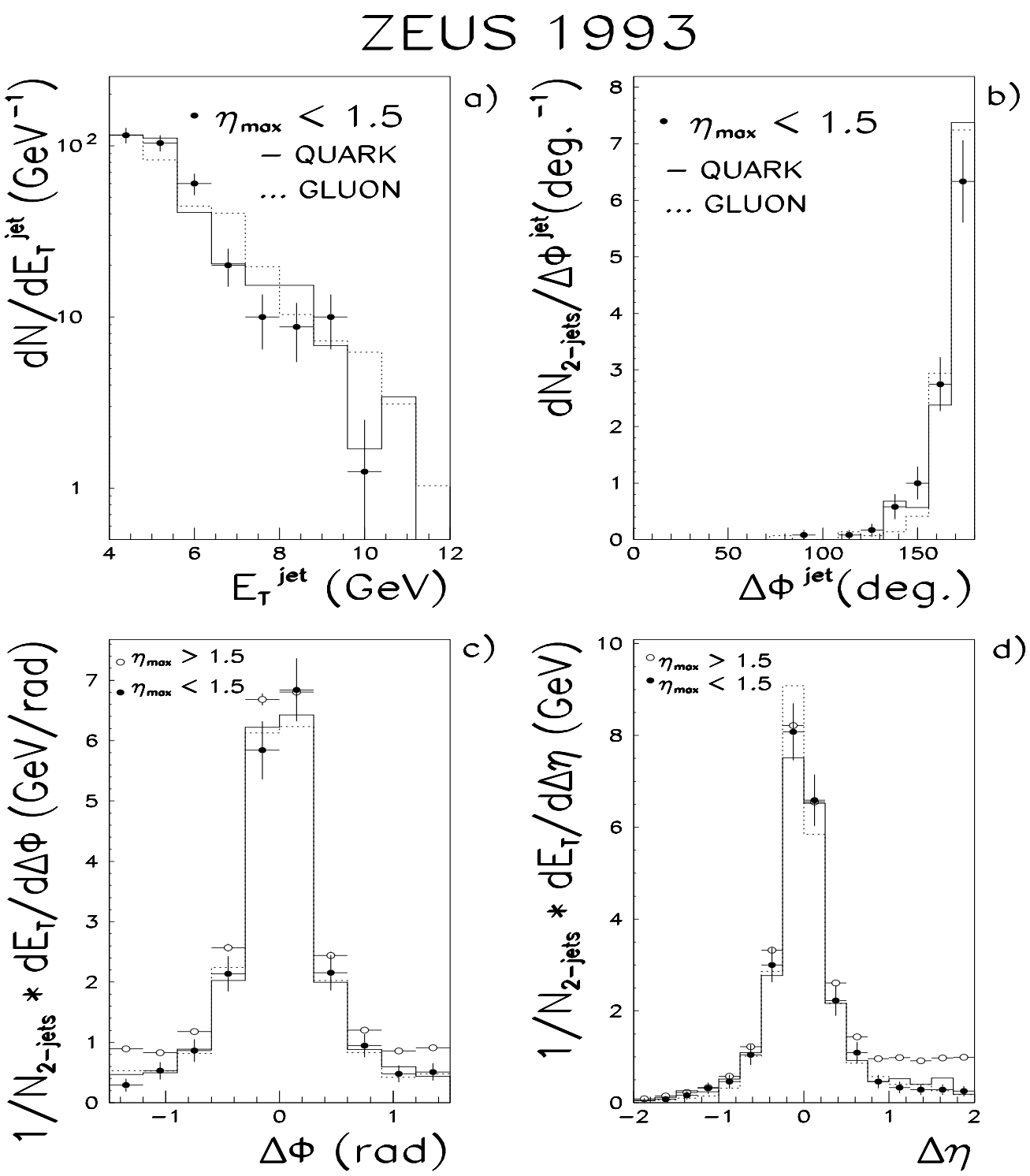

Figure 3:
(a) The transverse energy distribution of the jets in the two-jet sample in photoproduction with $\eta_{max} \leq 1.5$ along with the POMPYT predictions for a quarkonic (solid line) or gluonic (dotted line) pomeron.
(b) The $\Delta\phi^{jet}$ distribution for two-jet events in photoproduction with $\eta_{max} \leq 1.5$ along with a comparison with the POMPYT predictions as in (a).
(c, d) The transverse energy weighted profiles for jets with $\eta_{jet} < 0$ in photoproduction events with $E_T > 5$ GeV together with POMPYT predictions as in (a). Two samples are presented: one with $\eta_{max} \leq 1.5$ and the other with $\eta_{max} > 1.5$; (c) shows the azimuthal profiles and (d) shows the pseudorapidity profiles.

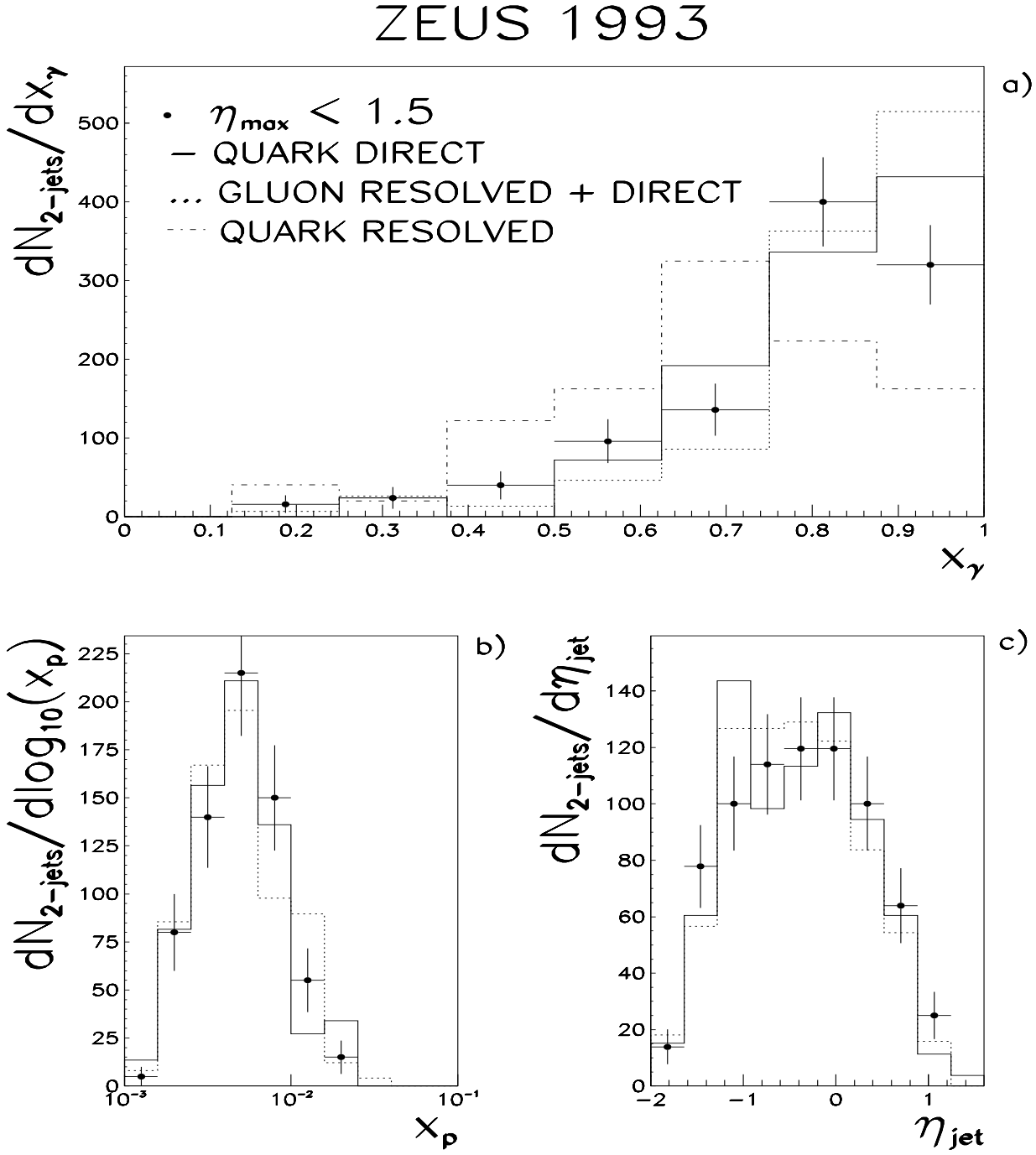

Figure 4:
(a) The x_γ distribution for photoproduction events with a large rapidity gap (dots) compared to POMPYT predictions. The solid line represents the direct photon interaction with a quarkonic pomeron. The dotted line denotes the sum of the direct and resolved interactions of the photon with a gluonic pomeron. Also shown are the results from POMPYT with a quarkonic pomeron using only the resolved photon processes (dash-dotted histogram). Each histogram has been normalised separately to the number of data events.
(b) The measured fraction of the proton momentum, x_p, entering the hard scattering for two-jet events, along with the POMPYT predictions for a quarkonic (solid line) or gluonic (dotted line) pomeron.
(c) The jet pseudorapidity distribution for the two-jet sample and for the POMPYT predictions, as in (b).